Overexpression of the *WAPO-A1* gene increases the number of spikelets per spike in bread wheat

Lukas M. Wittern[1†], Jose M. Barrero[4†], William D. Bovill[4], Klara L. Verbyla[4], Trijntje Hughes[4], Steve M. Swain[4], Gareth Steed[1], Alex A.R. Webb[1], Keith Gardner[3], Andy Greenland[3], John Jacobs[2], Claus Frohberg[2], Ralf-Christian Schmidt[2], Colin Cavanagh[5], Antje Rohde[2], Mark Davey[2‡] and Matthew A. Hannah [2‡*]

[1]Department of Plant Sciences, University of Cambridge, CB2 3EA, UK

[2]BASF, BBCC - Innovation Center Gent, Technologiepark 101, 9052 Ghent, Belgium

[3]National Institute of Agricultural Botany (NIAB), Huntingdon Road, Cambridge, CB3 0LE, UK

[4] Commonwealth Scientific and Industrial Research Organisation, Agriculture and Food, Black Mountain Science and Innovation Park, Canberra, ACT 2601, Australia

[5]BASF Australia Ltd., 28 Freshwater Place, 3006 Melbourne, Australia

† Shared first authors
‡ Shared last authors
*Corresponding author. Email: matthew.hannah@basf.com, Tel: +3292508598

Abstract

Two homoeologous QTLs for number of spikelets per spike (SPS) were mapped on chromosomes 7AL and 7BL using two wheat MAGIC populations. Sets of lines contrasting for the QTL on 7AL were developed which allowed for the validation and fine mapping of the 7AL QTL and for the identification of a previously described candidate gene, *WHEAT ORTHOLOG OF APO1* (*WAPO1*). Using transgenic overexpression in both a low and a high SPS line, we provide a functional validation for the role of this gene in determining SPS also in hexaploid wheat. We show that the expression levels of this gene positively correlate with SPS in multiple MAGIC founder lines under field conditions as well as in transgenic lines grown in the greenhouse. This work highlights the potential use of *WAPO1* in hexaploid wheat for further yield increases. The impact of *WAPO1* and SPS on yield depends on other genetic and environmental factors, hence, will require a finely balanced expression level to avoid the development of detrimental pleiotropic phenotypes.

Keywords: *WAPO1*, spikelets per spike (SPS), spike architecture, Multiparent Advanced Generation Intercross (MAGIC), wheat transgenics

Word count (not inc. Abstracts, Methods, References, Figure Legends): 4637 (of 4500)

Abstract: 166 (of 200)

Method: 1561 (of 1500)

References: 73 (of 60)

Tables and Figures: 7 (of 8)

Introduction

Grain yield is a highly complex trait which is the product of a network of inter-connected yield-component traits, such as tiller number, inflorescence architecture and the rate of grain filling, often with interdependencies and trade-offs involved[1]. Studying individual yield-component traits, particularly those with higher heritability such as spikelet number per spike (SPS)[2] can assist in reducing some of this complexity. As spikelets are specialized branches that produce grains, breeding for increased SPS could increase grain yield by increasing grain number and sink capacity.

SPS is affected by genes affecting flowering time through vernalization, photoperiod or earliness *per se (eps)* pathways: *VRN1*, *FUL2*, *FUL3*, *PPD1*, *VRN3*/*FT1*, *FT2*, *ELF3*[3–7]. Spring or winter growth habit is determined primarily by variation in the *VRN* genes. *PPD1* controls photoperiod-dependent floral induction, with the photoperiod insensitive allele *PPD-D1a* accelerating flowering, whilst *ELF3* is a minor effect *eps* gene. However, identification and characterization of major effect genes that increase SPS independently of these pathways has been limited so far.

The genetic dissection of grain yield and yield-component traits in hexaploid wheat is complicated by the compensatory effects of homoeologous genes. Their analysis in diploid model plants, such as rice, usually reveal QTLs with much higher effect sizes, e.g. 20-40% in rice vs 2-9% in hexaploid wheat[8]. Previous rice studies identified several genes involved in the regulation of panicle size and grain number and thus their orthologs provide a basis for studies in other cereals[9]. The rice gene *ABERRANT PANICLE ORGANIZATION 1* (*OsAPO1)* regulates panicle size, grain number[10,11] and yield[12,13] and higher expression of the *OsAPO1* transcript leads to more primary branches[11]. *OsAPO1* is syntenic with a major wheat SPS Quantitative Trait Locus (QTL) on chromosome 7AL in several bi-parental mapping populations and diversity panels[2,14–21] as well as a minor homoeologous QTL on 7BL[22,23].

More recently the *WHEAT ORTHOLOGUE OF APO1 (WAPO1)* has been proposed as the candidate gene for the SPS QTL on 7AL by multiple authors[24–26], and validated in tetraploid wheat using a combination of mutants and transgenic lines[27]. However, transgenic overexpression of *WAPO-A1* in multiple backgrounds of hexaploid wheat has not yet been reported, limiting our understanding of gene function, effect size, and pleiotropic effects for the more relevant hexaploid wheat breeding.

Multi-parental Advanced Genetic Inter-Crossed (MAGIC) populations are well suited for QTL mapping due to their high levels of allelic diversity and recombination[28–30]. Based on residual heterozygosity in the MAGIC populations, QTLs can be further validated and fine mapped through the development of Heterogeneous Inbred Families (HIFs). Selected HIFs will be isogenic at most loci in the genome, but still heterozygous for the region spanning the QTL of interest. The resulting segregating progeny will have properties similar to near-isogenic lines (hereafter named NILs) with and without the QTL of interest and are ideal genetic material to perform precise phenotyping and transcriptomic analysis, and to assess the allelic contributions to the trait of interest as well as for fine mapping and candidate causal gene identification[31].

In this study, we describe the functional validation of *WAPO1* in determining SPS in hexaploid wheat. We used two MAGIC populations across 14 site$^{\times}$year environments to identify two homoeologous SPS QTLs for 7AL and 7BL. Sets of contrasting NILs derived from HIFs segregating for the QTL on 7AL were used to validate and fine map the 7AL QTL, delivering a candidate gene *WAPO-A1* and its homoeologue *WAPO-B1*. For *WAPO-A1* we observed that increased expression in the spike in the NIAB MAGIC founder parents was positively correlated with SPS in the field. Therefore, our functional validation of

82 the *WAPO-A1* gene in hexaploid wheat used a transgenic approach in both low- and high-SPS genetic
83 backgrounds. This transgenic overexpression approach provided functional validation in hexaploid
84 wheat for the role of *WAPO-A1* expression level in determining the number of SPS. Furthermore, we
85 demonstrate that the increase in SPS in the transgenic lines is not always translated into an increased
86 number of seeds per spike and can lead to pleiotropic or compensation effects under our growing
87 conditions. The latter highlights the need to finely balance expression levels to achieve positive effects
88 on yield when applied in breeding.

Results

The CSIRO and NIAB MAGIC populations have a wide phenotypic spread in SPS

Twelve field trials using an 4-parent MAGIC population[32] from CSIRO were performed between 2011 and 2014 across three field sites in New South Wales, Australia (Yanco, Narrabri, Wallendbeen) and in a Greenhouse in Canberra (ACT, Australia). Two field trials using an 8-parent MAGIC population[28] from NIAB were performed in 2014 and 2015 in Cambridge, UK. Heritability of SPS across all trials and both populations was high, varying from 0.45 to 0.86 with a mean of 0.71 (Supplementary Table 1).

Both MAGIC populations showed transgressive segregation for SPS. In the 4-parent CSIRO population, recombinant inbred lines (RILs) had a mean SPS number ranging from 12.6 to 25.0 compared to 16.3 to 23.3 for the MAGIC parents. Yitpi and Chara were identified as having a reduced mean number of SPS when compared to Westonia and Baxter. On average the difference was at least one spikelet per spike between the CSIRO parents in the low and high SPS groups. The 8-parent NIAB population, RILs had mean SPS number ranging from 17.70 to 29.80 compared to 20.32 to 26.40 for the MAGIC parents. The NIAB MAGIC parents could also be broadly divided into high and low phenotype groups, with Soissons, Robigus and Brompton having a reduced SPS number compared to the other five MAGIC parents (Alchemy, Claire, Hereward, Rialto, Xi-19).

QTL mapping identified ten major SPS QTLs

QTL mapping was conducted using MPWGAIM[33] with a separate univariate analysis for each trial. In total, 203 marker-trait associations (MTAs) for SPS were identified across 12 trials for the CSIRO MAGIC population and 18 MTAs for SPS were identified across 2 trials for the NIAB MAGIC population (QTL significance $p < 0.05$) (Supplementary Tables 2&3). The CSIRO MTAs cluster into ten major QTLs that are highly significant (max. $-\log10(p) > 5$) and reproducible across at least two trials. For six of the identified QTL, we were able to assign candidate genes based on previously known allelic effects of flowering pathway genes, leaving four QTL that were initially not annotated. Of these, a SPS QTL on 7AL was observed most consistently at a high significance and was chosen for further downstream analysis (Table 1).

116 **Table 1: Overview of major SPS QTLs in the 4-parent CSIRO and the 8-parent NIAB MAGIC**
117 **populations and the underlying candidate genes.** QTLs for SPS from 12 trials with the 4-parent CSIRO
118 MAGIC population and two trials with the 8-parent NIAB population. QTL analyses were conducted
119 using whole genome average interval mapping using MPWGAIM[33]. For the NIAB MAGIC population a
120 genetic map adapted from Gardner et al., 2016[34] was used. For the CSIRO MAGIC population a
121 previously published map was used[33]. Genetic variance (%) and significance (-log10(p)) as calculated
122 by MPWGAIM[33]. *The QTL likely associated with *VRN-A1* was only observed in the CSIRO Greenhouse
123 studies, where vernalization did not occur. [$]Inferred from reported *VRN-B3* allele. Variety
124 abbreviations: Baxter (B), Chara (C), S (Soissons), W (Westonia), Y (Yitpi)

125

Chr	Genetic region (cM)		Genetic Variance (%)		Significance (-log10(p))		Studies (n)	Candidate gene	Effect
	Left	Right	Min	Max	Min	Max			
4-parent CSIRO MAGIC population									
2BS	159.29	165.35	1.6	11.8	1.94	10.9	7/12	*PPD-B1* [35]	Late allele in C increases SPS
2DS	0	9.61	15.9	30.2	22.21	38.71	5/12	*PPD-D1* [35]	Late allele in Y/B increases SPS
2DL	95.26	99.45	1.1	5.9	2	12.03	10/12	*Unknown*	
4AL	61.76	62.68	2.6	3.6	2.19	7.17	4/12	*Unknown*	
5AL	88.39	89.07	9.5	33.2	19.55	126.39	3/12*	*VRN-A1* [35]	Late allele in B increases SPS
5BL	97.75	99.74	1	4.5	1.54	9.03	7/12	*VRN-B1* [35]	Late allele in C increases SPS
5DL	131.11	152.57	1.5	8.8	2.17	17.76	8/12	*VRN-D1* [35]	Late allele in Y/C/W increases SPS
7AL	58.7	60.3	6.6	24.8	5.33	44.05	12/12	*WAPO-A1*	See Table 2
7BL	71.72	74.59	1.4	3.9	2.31	6.73	4/12	*WAPO-B1*	See Table 2
7BS	166.24	170.19	3.2	14.5	1.4	35.67	3/12	*VRN-B3* [36]	Early allele in B decreases SPS[$]
8-parent NIAB MAGIC population									
2DS	48.57	57.64	5	12.5	4.18	12.87	2/2	*PPD-D1* [35]	Early allele in S decreases SPS
7AL	257.05	257.21	19.2	33.8	42.1	66.17	2/2	*WAPO-A1*	See Table 2
7BL	144.34	144.5	1.5	1.5	2.05	2.05	1/2	*WAPO-B1*	See Table 2

126

127

128 Despite substantially different environmental conditions, the major QTL for SPS on 7AL was observed
129 in all 12 CSIRO trials and in two NIAB trials. This indicates that this QTL was environmentally and
130 genetically very stable (Supplementary Table 4). In the 4-parent CSIRO population, the 7AL SPS QTL
131 defined a 5.7Mb interval between 669.7Mb and 675.4Mb on the IWGSCv1.1 assembly, with a global
132 significance level of -log10(p)>5 across all 12 trials and mean genotypic variance explained of 13.6%.
133 Baxter and Westonia carry the high SPS genotype, with an average increase of 1.1 spikelets per spike
134 in the MAGIC RILs compared to the low SPS genotype (Yitpi, Chara), under these conditions. In the 8-
135 parent NIAB population the 7AL SPS QTL defined a narrower 2.3Mb interval between 672.0Mb and
136 674.3Mb. In the 2014 trial, the QTL explains a remarkable 33.8% of genetic variation in SPS within the
137 NIAB 8-way MAGIC population at a global significance level of -log10(p) 66.17. Alchemy, Claire,
138 Hereward, Rialto, Soissons, Xi-19 all carry the high SPS genotype, with an average increase of 2.1
139 spikelets per spike in the MAGIC RILs compared to the low SPS genotypes (Brompton, Robigus).

140 In addition to the major 7AL QTL for SPS, a homoeologous SPS QTL on 7BL with a smaller effect size
141 was also identified in both the 4-parent CSIRO and 8-parent NIAB populations (Table 1). In the 8-parent
142 NIAB population, this second QTL is located on a 4.9Mb interval (645.3 – 650.1Mb) directly
143 homoeologous to the 7AL QTL (-log10(p) = 2, Genetic Variance Explained (GVE) = 1.5%). Claire, Xi-19
144 and Soissons carry the high 7BL SPS parental genotype. Four of the 4-parent CSIRO trials also had a
145 7BL QTL mapping in the vicinity (642.5Mb – 655.0Mb) with Yitpi and Baxter carrying a high SPS
146 parental genotype (-log10(p)>2.3, mean GVE = 1.5%).

147 **Validation and fine mapping of the 7A SPS QTL using HIFs**

148 To validate and fine-map the 7AL QTL, four Heterogenous Inbred Families (HIFs) were derived from
149 selected F_7 RIL lines of the 4-parent CSIRO population containing heterozygosity in the QTL region.
150 These RILs were utilized to develop sets of NILs with contrasting presence of the 7AL SPS QTL.

151 Four NIL pairs (F0035, F0748, F1229, and F1570) showed consistent differences in SPS between the
152 contrasting alleles across the 7AL locus, thus validating the QTL (Figure 1A).

153 For two NIL pairs (F0748 and F1570) nearly all differences were statistically significant ($p < 0.05$).
154 Because the selected NILs carried the 7AL QTL genotypes of all four founder parents, the allelic effects
155 for each of the founders of the 4-parent CSIRO population could be determined. In addition, the SPS
156 region was further delimited from 5.7Mb to an interval of 2.2Mb by NIL pairs F0035 and F1570 (Figure
157 1B).

158 Additional phenotyping revealed the high SPS lines in each NIL pair also showed an increase in Grain
159 number per spike in most cases, albeit mostly insignificant, (Supplementary Figure S1) and no
160 differences in heading date exceeding 0.5 days were observed (Supplementary Figure S2).

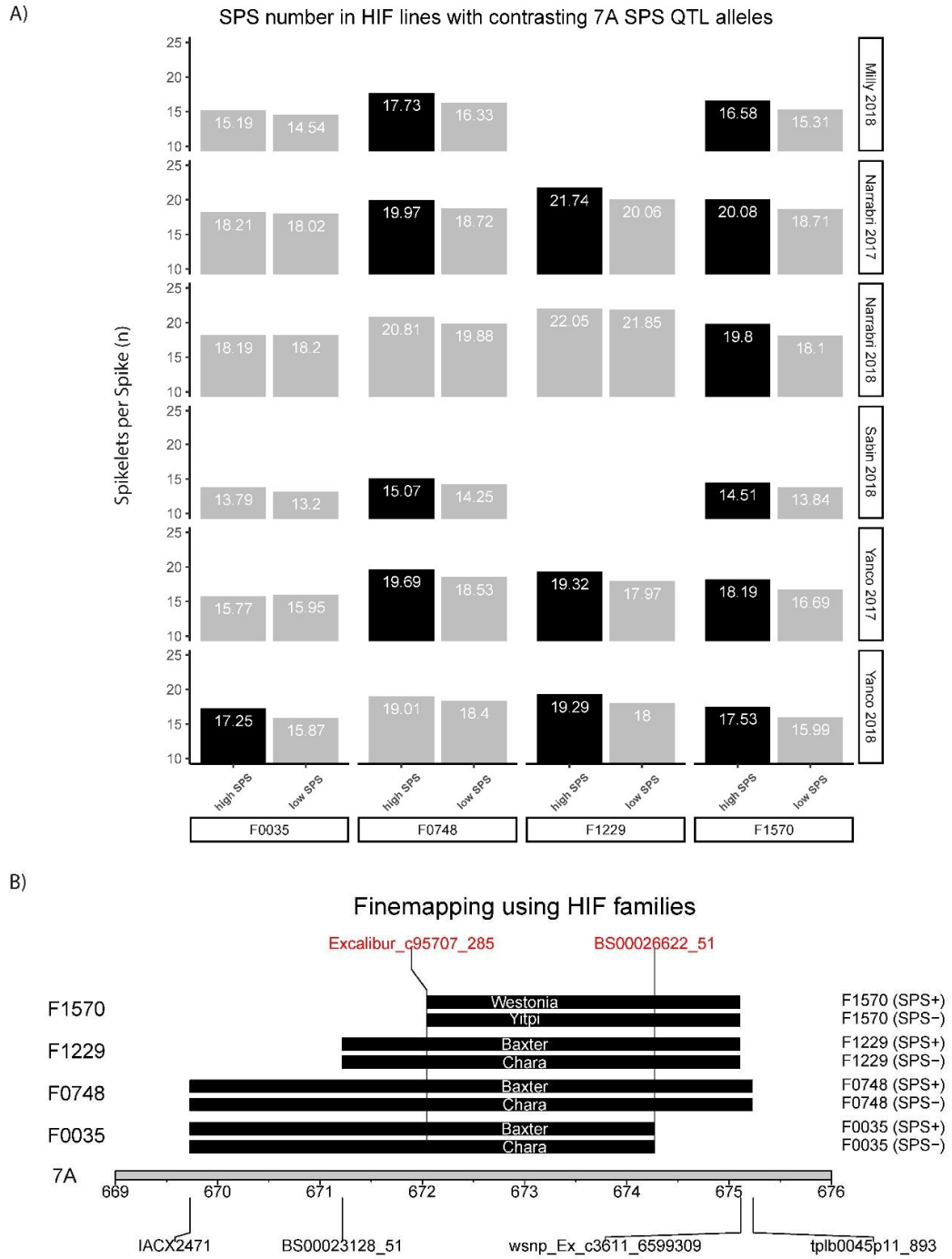

Figure 1: Validation and fine mapping of the 7A SPS QTL using HIF families derived from the CSIRO 4-way MAGIC population. A) Summary of differences in mean SPS values across NIL pairs for the 7AL SPS QTL. Black fill indicates a significant increase ($p<0.05$) between NIL pairs. B) Finemapping using HIF families. Contrasting founder genotypes in the NIL pairs are shown. The common QTL region is delimited by markers Excalibur_c95707_285 and BS00026622_51. The NIL pairs were phenotyped at four locations in France, the USA and Australia during 2017 and 2018 (6 site^{x}year combinations).

Identification of *WAPO-A1* and *WAPO-B1* as homoeologous candidate genes for SPS

The QTL region delineated using the HIFs on 7AL contained twenty genes. Both the 7AL and 7BL QTL identified in the NIAB and CSIRO MAGIC populations are syntenic to rice chromosome 6 (Figure 2). Within these three homoeologous or syntenic QTL regions, four conserved orthologous protein groups were identified*: TraesCS7A02G480100/TraesCS7B02G382300/OsHMA9*, *TraesCS7A02G481500/TraesCS7B02G383900/OsAAH*, *TraesCS7A02G481600/TraesCS7B02G384000/OsAPO1* and *TraesCS7A02G482000/TraesCS7B02G384200/Os06g0665100.*

OsHMA9 is a metal-efflux protein and *OsAAH* an allantoate deiminase. Neither have previously been linked to SPS phenotypes[37,38].

OsAPO1 is an F-box protein that had previously been shown to improve rice yield, primary rachis branching and lodging resistance as the causal gene of *qPBN6*[39,40] and *SCM2* QTL in rice[12]. The wheat orthologues of *OsAPO1* on 7AL and 7BL (*WAPO-A1* and *WAPO-B1*) were thus identified as good candidate genes for the 7AL and 7BL SPS QTLs. We also confirmed that no SPS QTLs were detected in the *WAPO-D1* genomic region. *WAPO-A1* and *WAPO-B1* genes and *WAPO-A1* promoter sequences for Fielder, Chinese Spring, Robigus and Claire were obtained from public resources[41–43]. *WAPO-A1* and 5kb of upstream promoter sequence in Yitpi, Baxter, Chara and Westonia were obtained by Sanger Sequencing (GenBank ON210994-ON210998).

Sequence alignments showed that the high SPS *WAPO-A1* allele carries a 115bp promoter deletion and two amino acid changes (C47F and D384N). Based on recent *WAPO-A1* nomenclature[24] we reclassified our alleles accordingly (Table 2). All the assigned *WAPO-A1* alleles are consistent with the observed founder effects in both MAGIC populations for the 7AL SPS QTL.

We also classified *WAPO-B1* alleles based on recent nomenclature[22] (Table 2). All assigned *WAPO-B1* alleles are also consistent with the observed founder effects except for Soissons, which has a high SPS founder effect on 7BL, while carrying the low SPS *WAPO-B1.hap1* allele. Westonia carries the *WAPO-B1.hap3* allele, previously reported to carry a frameshift mutation/premature stop codon[22]. Based on our alignments and the protein sequence of previous *WAPO-B1* gene model TRIAE_CS42_7BL_TGACv1_578478_AA1895640.1 we believe that this gene model is annotated incorrectly (Supplementary Figure S3) and that as a result, this InDel is unlikely to cause a premature stop as it falls into the 5' UTR of *WAPO-B1*. This observation would be consistent with the fact that *WAPO-B1.hap3* only has an intermediate SPS phenotype across four trials.

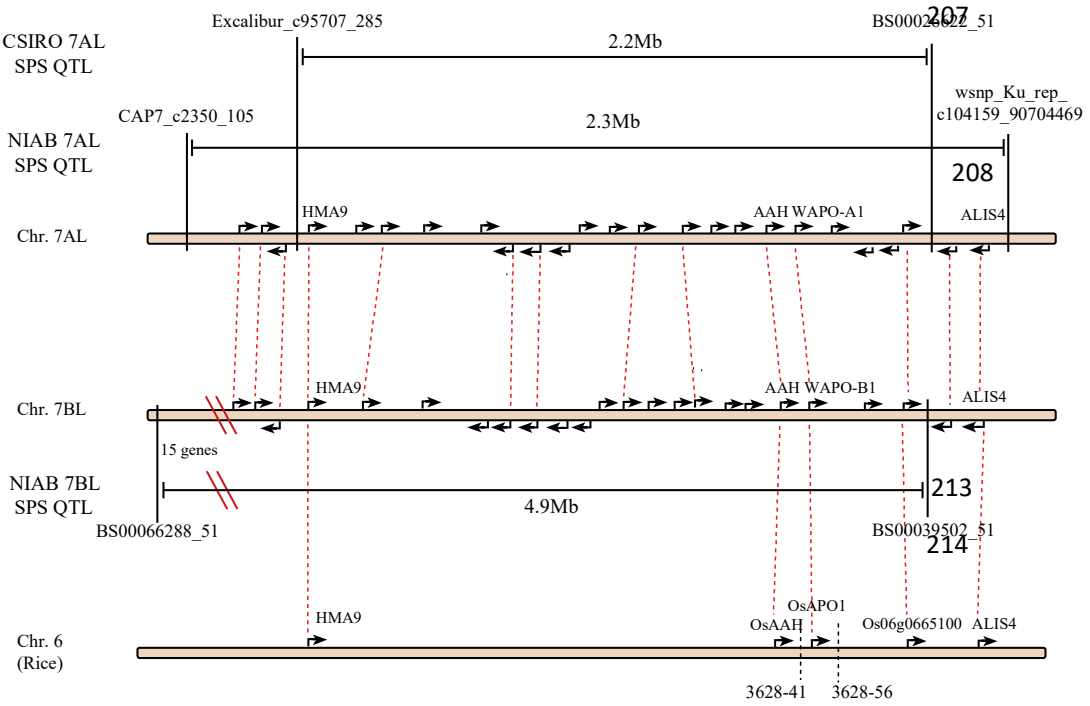

Figure 2: Syntenic relationships between the 7AL and 7BL SPS QTLs in the 4-parent CSIRO MAGIC population and the 8-parent NIAB MAGIC population and the rice SCM2/qPBN6 QTL[12,39]. Arrows indicate locations of IWGSCv1.1. gene models obtained from Ensembl Plants release 51. Dashed red lines indicate homoeologous and orthologous relationships as defined by Ensembl Plants 51. Gene descriptions from Ensembl Plants 51 have been added where available. Physical distances are not drawn to scale.

227 **Table 2: Founder effects and *WAPO-A1* and *WAPO-B1* alleles of NIAB and CSIRO MAGIC parents.**
228 Founder effects classified based on MPWGAIM predictions. *WAPO-A1* and *WAPO-B1* alleles classified
229 according to Kuzay et al., 2019[24] and Corsi et al., 2021[22]. *Founder phenotypic effects for Fielder and
230 Chinese Spring (CS) are inferred based on genome sequence information since they are not MAGIC
231 founder parents. Detailed variant calls presented in Supplementary Table S5.
232

Variety	***7A SPS QTL***		***7B SPS QTL***	
	Founder effect at 7AL	***WAPO-A1* allele**	**Founder effect at 7BL**	***WAPO-B1* allele**
Yitpi	low SPS	*WAPO-A1a*	high SPS	*WAPO-B1.h2*
Baxter	high SPS	*WAPO-A1b*	high SPS	*WAPO-B1.h2*
Chara	low SPS	*WAPO-A1a*	low SPS	*WAPO-B1.h1*
Westonia	high SPS	*WAPO-A1b*	intermediate SPS	*WAPO-B1.h3*
Alchemy	high SPS	*WAPO-A1b*	low SPS	*WAPO-B1.h1*
Brompton	low SPS	*WAPO-A1a*	low SPS	*WAPO-B1.h1*
Claire	high SPS	*WAPO-A1b*	high SPS	*WAPO-B1.h2*
Hereward	high SPS	*WAPO-A1b*	low SPS	*WAPO-B1.h1*
Rialto	high SPS	*WAPO-A1b*	low SPS	*WAPO-B1.h1*
Robigus	low SPS	*WAPO-A1a*	low SPS	*WAPO-B1.h1*
Soissons	high SPS	*WAPO-A1b*	high SPS	*WAPO-B1.h1*
Xi-19	high SPS	*WAPO-A1b*	high SPS	*WAPO-B1.h2*
CS*	high SPS	*WAPO-A1b*	high SPS	*WAPO-B1.h2*
Fielder*	high SPS	*WAPO-A1b*	low SPS	*WAPO-B1.h1*

233
234
235

236 ***WAPO-A1* expression in the field is correlated with SPS**

237 To investigate if the expression of *WAPO-A1* in wheat is correlated with SPS in the field we collected
238 samples from tiller dissections of the eight NIAB MAGIC parents from a 2017 field nursery at growth
239 stage GS32[44], because wheat-expression.com[45] data suggests that *WAPO1* homoeologous are
240 expressed in the spike at this developmental stage. Expression analysis using qRT-PCR confirmed that
241 higher *WAPO-A1* expression in wheat inflorescences is correlated (R^2 = 0.77) with increased SPS
242 (Figure 3). The low expression of *WAPO-A1* in Soissons may be a result of the presence of the *Ppd-D1a*
243 allele in this variety, which accelerates flowering time, so we possibly missed the expression peak of
244 *WAPO-A1*.

245

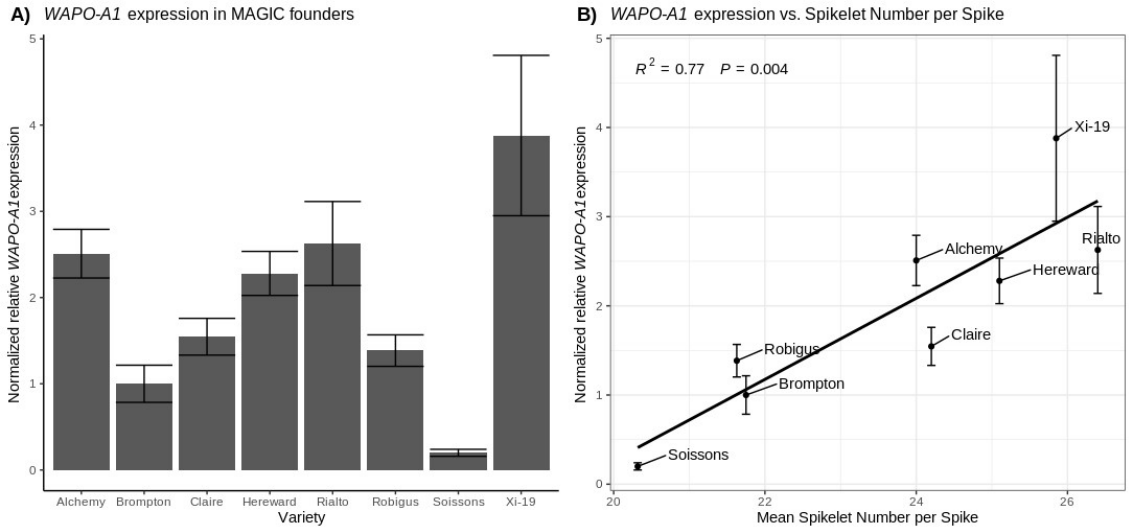

246

247

248 **Figure 3: *WAPO-A1* expression is correlated with spikelet number per spike.** All samples were
249 collected at GS32 apart from Soissons which at the collection date had advanced to GS34. A)
250 Expression of *WAPO-A1* transcript relative to the housekeeping genes *TaRP15*[46] and *Ta2291*[47]and
251 normalized to *WAPO-A1* expression in Brompton. B) Regression of expression of *WAPO-A1* (n = 3) on
252 mean SPS for the MAGIC Founder lines (n=20) in the 2014 field trial. Error bars are SEM.

253

254 **Transgenic complementation of the *WAPO-A1a* allele with *WAPO-A1b* leads to increased SPS and**
255 **spike length**

256 To functionally validate the *WAPO-A1* candidate, Yitpi, carrying the low SPS *WAPO-A1a* allele, was
257 complemented with the native high SPS *WAPO-A1b* allele and promoter from Westonia (~8Kb
258 genomic fragment, see methods) using Agrobacterium mediated transformation. Six sets of T_2 single-
259 insertion homozygous lines next to their respective null-segregant control line were grown in the
260 glasshouse and phenotyped (Figure 4A, 4B and Supplementary Figure S4).

261 Four out of six transgenic lines showed an increase in SPS compared to their null segregant.
262 Homozygous T_2 lines #5 and #3 displayed the strongest phenotype reaching more than 27 and 25 SPS,
263 respectively, as compared to 23 in their null segregants. Homozygous plants from lines #9 and #12
264 displayed a gain of about one SPS, while lines #4 and #7 did not show a significant difference in SPS
265 compared to their null segregants. The number of SPS in a non-transformed Yitpi control was similar
266 to the null-segregant lines (Figure 4B).

267 Samples of developing spikes at GS32 were collected from these lines for gene expression analysis
268 using qRT-PCR (Figure 4C), which revealed a strong correlation between the level of *WAPO-A1*
269 expression and the number of SPS and spike length (Figure 4D, E). These results are consistent with a
270 causal, positive correlation between *WAPO-A1* expression and the number of SPS and spike length.

271

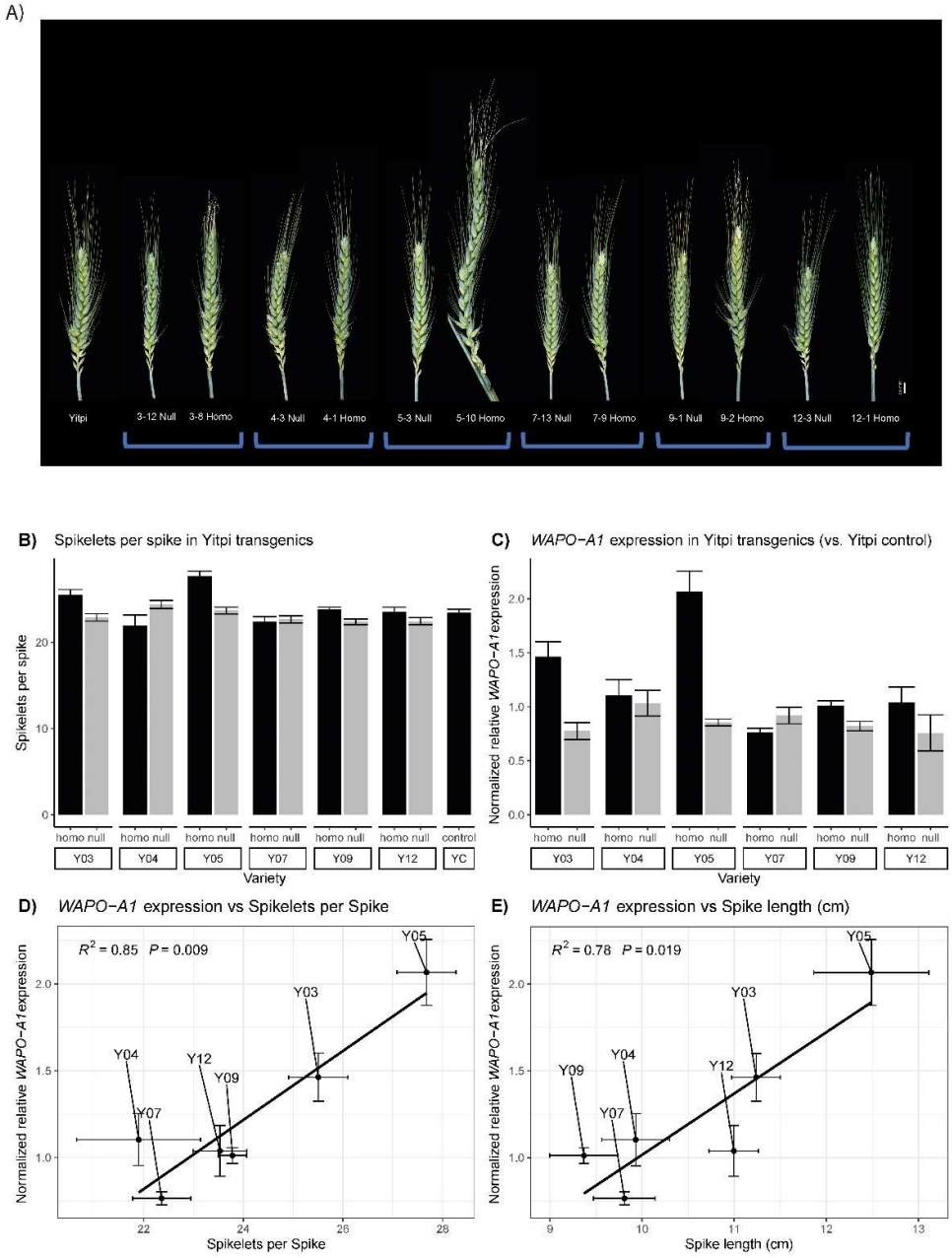

Figure 4: Spike phenotypes and WAPO-A1 expression in Yitpi transgenic and control lines. A) Representative spikes from transgenic lines, their null-segregants and non-transformed Yitpi plants. We observed the appearance of infertile basal spikelets in all genotypes although they were more common in transgenic plants. The presence of paired-spikelets was similar across all type of plants. B) Mean SPS number phenotyped at maturity in transgenic lines, their null-segregants and non-transformed Yitpi plants. C) Gene expression was assayed in developing spikes dissected at GS32 and normalized to the Yitpi WT control. The means and SEM of three biological replicates are shown. D) Regression of expression of *WAPO-A1* on SPS for the six transgenic lines carrying the Westonia *WAPO-A1* transgene. E) Regression of *WAPO-A1* expression on Spike length. For SPS and Spike length, 50 spikes (5 spikes x 10 plants) of each genotype were analysed

SPS levels can be increased above those conferred by the native *WAPO-A1b* allele

To determine if SPS and seeds per spikelet could be increased beyond the levels of the high SPS *WAPO-A1b* allele, we also transformed Fielder, which already contains a native high-SPS *WAPO-A1b* allele, with the native high-SPS *WAPO-A1b* allele and promoter from Westonia. We generated five independent primary transgenics in the Fielder background and isolated three single-insertion lines, for which we identified homozygous T_2 and null-segregants for phenotypic analysis of SPS, empty basal spikelets and seeds per spike.

All three transgenic lines showed an increased number of SPS in comparison to the nulls and the number of SPS was strongly correlated with the level of transgene expression (Figure 5, Supplementary Figure S5). These results further validated the conclusion that SPS number is closely correlated with WAPO-A1 expression levels. It also demonstrates that it is possible to increase SPS number beyond the levels determined by the native high SPS allele alone.

The Fielder control lines have fewer SPS (SPS = 17.02) than the Yitpi control (SPS = 23.44), despite carrying the favourable *WAPO-A1b* allele. This difference in SPS between the two cultivars could be explained by different photoperiod responses. Fielder carries the photoperiod insensitive *PPD-D1a* allele while Yitpi carries the photoperiod sensitive *PPD-D1d* allele, known to increase SPS[4].

Importantly, all the homozygous transgenic lines of Fielder, but not Yitpi containing the native high SPS *WAPO-A1b* transgene had spikes displaying a "compact head" phenotype (Supplementary Figure S6), which was also previously described[27]. This phenotype was observed in all three Fielder families in the homozygote T_2 lines but was not seen in the null-segregants.

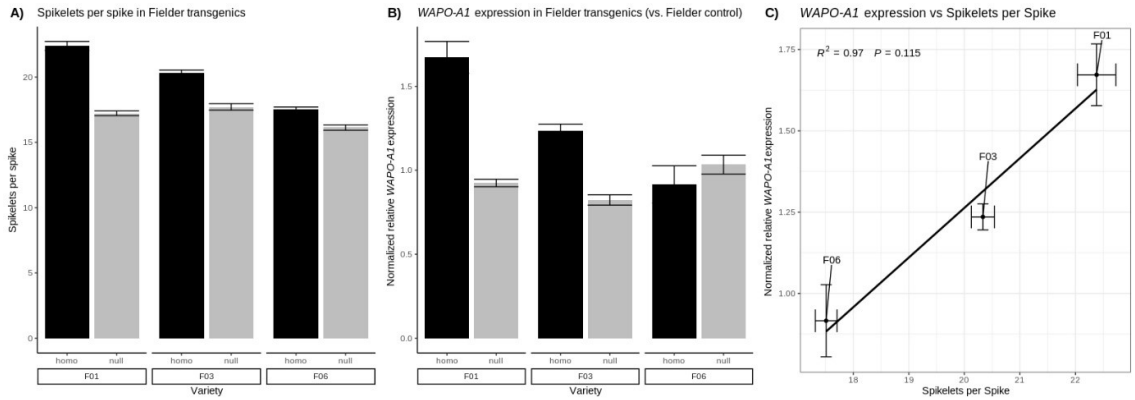

Figure 5: WAPO-A1 expression analysis in Fielder transgenic and control lines. A) Mean SPS of transgenic and null-segregants of plants phenotyped at maturity; B) Gene expression was assayed in developing spikes dissected at GS32. Expression is normalized to the Fielder WT control. C) Regression of expression of *WAPO-A1* on SPS for the transgenic lines. Means and SEM of three biological replicates are shown.

Increases in *WAPO-A1* expression may cause pleiotropic effects

315 In hexaploid wheat an increase in infertile spikelets in *WAPO-A1b* lines compared to *WAPO-A1a* has
316 previously been described[22,26]. In Kronos, a tetraploid wheat, a reduction in spike fertility has also been
317 reported[27], in lines containing additional WAPO-A1 transgene copies. In our studies the transgenic
318 lines with higher levels of *WAPO-A1* expression show an increased number of empty basal spikelets
319 (Supplementary Figure S7). This was especially pronounced in the highest expressing lines, both in
320 Yitpi (T_2 line #5) and Fielder (T_2 line #1). Similar to phenotypes previously described in tetraploid wheat
321 (Kronos) *WAPO-A1* overexpression lines[27] we observed one or two malformed florets at the base of
322 some spikes of the transgenic lines. The phenotypic alterations are indicative for developmental
323 disorders like homeotic transformations or failed organ development (Supplementary Figure S8).

324 In rice, lines with increased *OsAPO1* expression reveal a suppression of tiller outgrowth[11]. Similarly,
325 we observed a negative association between tiller number and *WAPO-A1* expression across our
326 transgenic Yitpi lines in the greenhouse pot experiment (Supplementary Figure S7). However, the null
327 segregants also showed variability in this trait meaning the decrease was only significant in one line
328 (T_2 line #5).

329 **Increased SPS in transgenic lines does not translate into equivalent increases in seed yield**

330 Under our greenhouse conditions we could not measure a clear benefit in yield (as seeds per spike or
331 per plant) associated with transgene expression (Supplementary Figure S4), either due to the
332 pleiotropic phenotypes described above or potential source limitations under these growth
333 conditions.

334 The transgenic Yitpi line with the highest transgene expression and number of SPS (T_2 line #5, T_2 line
335 #3) showed a clear penalty in both seeds per spike and seeds per plant. We also observed an extreme
336 branching phenotype and floral defects in a small proportion of the spikes developed by Yitpi T_2 line
337 #5 (Supplementary Figure S8). In fact, the spikes were often so long that they did not fully emerge
338 from the underlying leaf sheath, and the florets inside were often infertile (Figure 4A). Taken together,
339 our data indicate, that a too high expression of *WAPO-A1* reveals a rather negative effect on seed
340 production.

341 However, lines with a lower increase of the transgene and a resulting smaller increase in SPS such as
342 Yitpi T_2 Line #12 (*WAPO-A1* expression increase 37%; Seeds per spike increase 11%) and Fielder T_2 line
343 #3 (*WAPO-A1* expression increase 50%; Seeds per spike increase 21%) indicated that increases in seeds
344 per spike could be observed, suggesting that one can select an optimal range of *WAPO-A1* expression
345 levels to achieve the desired phenotypic and yield effects.

346

347 ## Discussion

348 **MAGIC populations are well suited for QTL dissection**

349 The use of two separate MAGIC populations across 14 site×year environments enabled us to capture
350 a wide range of genetic and phenotypic variation and to identify homoeologous SPS QTL on 7AL and
351 7BL. The additional recombination present in MAGIC populations allowed for improved mapping
352 resolution which aided the direct identification of candidate genes, as was the case with the NIAB
353 MAGIC population, or via the generation of HIF lines[31]. This pipeline for candidate gene discovery via
354 HIF lines derived from MAGIC populations is repeatable using other yield-component traits.

355 MAGIC populations can also reveal the effects of stacking of favourable alleles through transgressive
356 segregation[48] as well as epistatic effects[49]. Within the 4-parent CSIRO population alleles at the *Ppd-*
357 *D1*, *PPD-B1*, *VRN-A1*, *VRN-B1* and *VRN-D1* loci are segregating in addition to *WAPO-A1* and *WAPO-*
358 *B1*[32,35]. In addition to *WAPO-A1* and *WAPO-B1,* within the 8-parent NIAB population *Ppd-D1*, *ELF3-B1*
359 and *ELF3-D1* are also segregating [4,7,28,50]. All of these loci were identified as significant SPS QTL in the
360 respective populations with the exception of *ELF3-B1* and *ELF3-D1,* which may be due to their minor
361 effect on SPS or due to more complex environmental interactions of *ELF3*[51].

362 **Overexpression of *WAPO-A1* in hexaploid wheat increases SPS**

363 The *WAPO-A1* gene has been proposed as the candidate gene for a major QTL for SPS on 7AL mapped
364 in several populations[22–26] and the *WAPO-B1* gene as a candidate for a smaller QTL for SPS on 7BL[22].
365 Recently, [27]Kuzay et al., 2022 demonstrated, using CRISPR-generated mutants and transgenic plants,
366 the role of *WAPO-A1* and *WAPO-B1* in determining SPS in tetraploid wheat.

367 Here, we provide functional evidence in hexaploid wheat for a similar role of the *WAPO-A1* gene in
368 determining SPS in a dose dependent manner. We have generated two sets of transgenic lines to test
369 the effect on supplementing cultivars carrying either the low-SPS *WAPO-A1a* or the high-SPS *WAPO-*
370 *A1b* alleles with a *WAPO-A1b* allele from a high-SPS cultivar (Westonia). In both sets of transgenic
371 lines, we observed a positive correlation between *WAPO-A1* expression and the number of SPS, which
372 is consistent with variation in *WAPO-A1* being responsible for the observed QTL. [27]Kuzay et al., 2022
373 provided strong evidence for a role of *WAPO-B1* in determining SPS, by a reduced number of SPS
374 present in *wapo-b1* mutants. However, it was previously reported that overexpression of *WAPO-D1*
375 in the elite hexaploid variety KN199 had no effect on spike phenotypes[19]. Different *WAPO1*
376 homoeologues may therefore have different effects on SPS.

377 At the molecular level, *WAPO-A1* increases the expression of B-Class and C-Class MADS box genes,
378 which affect lodicules, stamen and carpel development[52]. This is a possible cause behind the floral
379 abnormalities and reduced fertility observed in both the transgenic Yitpi and Fielder lines. In the
380 Fielder transgenics we also observed a compact spike phenotype, which indicates that the
381 overexpression of *WAPO-A1* in these lines alters spike development in several ways. Similar
382 phenotypes in the florets and spikes have been reported in transgenic lines overexpressing the *WAPO-*
383 *A1* gene in the tetraploid wheat cv Kronos[27].

384 In transgenic lines displaying a low level of expression of the *WAPO-A1* transgene, and a small increase
385 in SPS, we observed an increase in the number of seeds per spike (Yitpi line #12 and Fielder line #3).
386 This is in line with the idea that a subtle rather than a strong increase of *WAPO-A1* expression levels
387 could be associated with increased grain number. This is similar to the situation in rice in which *SCM2*,

388 a weaker allele of *OsAPO1* compared to *Ur1*, has been reported to increase spikelet numbers without
389 reducing panicle number[12]. For commercial application of transgenic lines, further validation of the
390 positive yield component phenotypes observed in transgenic lines with modest increases in *WAPO-A1*
391 expression in a replicated field trial environment will be required. The long timelines, high costs and
392 current lack of commercial transgenic traits in wheat also represent significant challenges for product
393 development.

394 ***WAPO-A1* activity is finetuned via interconnected, developmental pathways**

395 QTL mapping in the two MAGIC populations revealed large phenotypic effects of *PPD-D1a* and *VRN-*
396 *A1a* (and likely *VRN-B3* as well) on the number of SPS. More minor but significant effects on SPS from
397 *PPD-B1a*, *VRN-B1a* and *VRN-D1a* were also observed. The MAGIC populations studied here thus form
398 an excellent platform to identify the genetic backgrounds that optimise the SPS, and grain number
399 potential associated with *WAPO-A1b* for specific environments.

400 *PPD1*, *VRN1* and *VRN3* all influence the timing of transition from vegetative to inflorescence meristem
401 (IM) and from IM to terminal spikelet[3–5,53]. Later transitions are associated with increased SPS[53], either
402 linked to the duration or resources available for development. This would explain the low SPS
403 observed for Soissons, carrying the early *PPD-D1a* allele, despite having the high-SPS *WAPO-A1b* allele.
404 Similarly, in our greenhouse experiments Fielder (*WAPO-A1b*, *PPD-D1a*) also had fewer SPS than Yitpi
405 (*WAPO-A1a*, *PPD-D1d*). *WAPO-A1* native alleles on the other hand have not been reported to cause
406 large changes in flowering time in field trials[25,53] and while transgenic expression delayed flowering,
407 CRISPR and EMS mutants had no significant effects[27].

408 Our results show that the *WAPO-A1b* allele has a larger effect on the number of SPS in the winter
409 wheat NIAB MAGIC population (+2.1 SPS) compared to the spring wheat CSIRO MAGIC population
410 (+1.1 SPS; *VRN-A1a* and/or *VRN-B1a* and/or *VRN-D1a* present, see Table 1). An epistatic interaction
411 between *WAPO-A1*, *VRN-D3*, *PPD-B1* and *Qsn.csu-6B* has recently been described[53]. These data
412 together support the conclusion that the phenotypic effect of *WAPO-A1* alleles on SPS is finetuned by
413 the timing of developmental transitions and the genetic constitution of *PPD1*, *VRN1 and VRN3.*

414 The interactions of *WAPO-A1b* with flowering pathways can also be discussed at the molecular level.
415 *PPD1*, *VRN1* and *VRN3*/*FT* form part of a signalling cascade that leads to the upregulation of *SOC1-1*
416 and *LFY*[54]*.* The orthologue of *LFY* is *OsAPO2*[55] in rice and *HvLEAFY* in Barley[56], which interact with the
417 *WAPO1* orthologues *OsAPO1* or *HvUFO,* respectively. OsAPO1 and OsAPO2 form a regulatory module
418 together with LARGE2[32]. *OsAPO2* has also been previously shown to be transcriptionally regulated by
419 *SP3*[57] in rice. Together the *WAPO1* pathway genes are expressed in the IM and lateral meristems and
420 extend IM maturation and control spikelet meristem identity acquisition[58]. This may also explain the
421 extreme branching phenotype observed in some spikes of the transgenic Yitpi T_2 line #5.

422 To further elucidate the complexity of these regulatory networks, further work should focus on
423 determining epistatic relationships between the identified QTLs at the phenotypic level as well as
424 relating this to more comprehensive studies of expression changes and molecular interactions in
425 different genetic backgrounds.

426 ***WAPO1* breeding applications**

427 Increasing SPS is a potential path to increasing seeds per spike, grain number and ultimately yields.
428 *PPD1* and *VRN1* have already been deployed to locally adapt cultivars to geographic adaptation zones

429 and due to their importance for local adaptation it can be assumed that there would likely be extensive
430 trade-offs in their use in improving SPS. *WAPO-A1b* on the other hand is potentially valuable for wheat
431 breeders as it can increase SPS in locally adapted varieties without having strong impacts on flowering
432 time.

433 However, the increased number of SPS found in most of the transgenic lines is not always translated
434 in an increased number of seeds per spike. Perhaps, under our glasshouse growing conditions, the
435 plants did not have sufficient resources to fill the extra spikelets, which might be especially relevant
436 in pot experiments, where a large number of tillers and spikes per plant is formed as compared to the
437 situation in dense canopies under field conditions. Additionally, strong overexpression of *WAPO-A1*
438 produces some defects during floret or seed development.

439 These results align with those of other publications that report on the pleiotropic effects of *WAPO-*
440 *A1b,* including reduced spike fertility[26] and increased seeds per square meter but reduced TGW[15]. As
441 previously proposed[24], our results imply that *WAPO-A1b* promotes an increase in sink capacity which
442 may require introgression into high-biomass productive varieties and cultivation under conditions that
443 support high yield potential. The observed trade-offs are not unique to *WAPO1* and have been shown
444 in other genes that increase sink capacity such as *FT2*[59] and *FUL2*[3]. In rice it has also been reported
445 that Os*APO1* increases yield[13], but that the effect on yield is source dependent[60] and dependent on
446 gene expression levels as described above.

447 It might be possible to overcome these trade-offs by stacking *OsAPO1*/*WAPO-A1* with genes that have
448 complementary phenotypic effects, and some promising examples have been reported in both rice
449 and wheat. For example, stacking *WAPO-A1* with *GNI-A1* and *qGSNP-A-5A* to further increase SPS
450 without reducing TGW was possible in a Japanese dihaploid wheat population[14].

451 An alternative approach may be to exploit genes known to interact at the molecular level. In rice it
452 was recently shown that that OsAPO1 physically interacts with OsAPO2 and a HECT-domain E3
453 ubiquitin ligase LARGE2/OsUPL2. LARGE2 modulates the protein stability of OsAPO1 and OsAPO2[61].
454 Extrapolating from these results in rice, further finetuning of WAPO1 activity and resulting SPS and
455 seed number might be possible in wheat through posttranscriptional mechanisms and may help to
456 overcome the constraints due to the limited number of *WAPO-A1* alleles that have currently been
457 identified.

458 **Conclusion**

459 This study has provided functional validation in hexaploid wheat for the role of *WAPO-A1* in
460 determining SPS. We demonstrated that the expression level of this gene in MAGIC lines under field
461 conditions as well as in transgenic lines in the greenhouse is positively correlated with the number of
462 spikelets per spike. We also identified potential pleiotropic effects of excessive *WAPO-A1* expression.
463 Future work can focus on identifying additional existing or novel *WAPO1* alleles that have an optimized
464 level of expression and protein activity or identifying pathways and genes that can be used to optimize
465 the expression of *WAPO1* or that have complementary phenotypic effects. The optimal activity of
466 *WAPO-A1* resulting into yield gains can be expected to be dependent on the yield potential of the
467 environment and agronomic practice.

468 ## Methods

469 **Plant Materials**

470 The founder parents for the NIAB and CSIRO wheat MAGIC populations were selected based on wide
471 genotypic and phenotypic diversity.

472 The 4-parent CSIRO MAGIC population founders are spring wheat cultivars from Australia (Yitpi,
473 Baxter, Chara and Westonia)[32].

474 Six of the NIAB MAGIC population founder parents are winter wheat cultivars from the United
475 Kingdom (UK) (Alchemy, Brompton, Claire, Hereward, Rialto, Robigus) and one from France (Soissons)
476 and one is a facultative spring variety (Xi-19)[28].

477 All plant material used in this study was derived from commercially released wheat varieties that
478 were obtained and used in accordance with applicable institutional, national and/or international
479 regulations**.**

480 **SPS Phenotyping**

481 For the 4-parent CSIRO MAGIC population, F_6 derived RILs were grown in partially replicated trials[62]
482 (partial replication rate of 1.2 - 1.5): 1080 lines were grown in a Greenhouse (Canberra, ACT, Australia,
483 CSIRO Black Mountain Site; 2011(F_9), 2012(F_{10}), 2013(F_{10})), 1009, 960 and 1008 field plots were grown
484 in Narrabri (New South Wales, Australia; 2012(F_{10}), 2013(F_{10} & F_{11}), 2014(F_{12})), 1500, 1800 and 1009
485 field plots in Wallendbeen (New South Wales, Australia; 2011(F_9), 2012(F_{10}), 2013(F_{10})) and 1120, 1920
486 and 912 in Yanco (New South Wales, Australia; 2012(F_{10}), 2013(F_{10}), 2014(F_{12})). Three representative
487 wheat ears were collected from each plot and the spikelets per spike (the total number of rachis nodes
488 plus the terminal spikelet) were hand counted starting at the bottom of each spike.

489 Additionally, a fully replicated trial of 784 F_7 8-parent NIAB MAGIC RILs and the eight founders was
490 grown at the NIAB experimental farm in Cambridge, UK during the 2013/2014 field season. Ten
491 representative wheat ears were collected from 1000 of the 1600 plots in the field and dried at room
492 temperature. Collection was done in a partially replicated design with 200 RILs and the MAGIC
493 founders collected in duplicate. In 2014/2015 a nursery of 1091 F_8 MAGIC lines and the founders was
494 screened for SPS as described above by collection of six representative wheat ears.

495 Selected F_{12}, F_{13} NIL sets were grown in 2017 and 2018 in Narrabri and Yanco, NSW, Australia and in
496 2018 in Sabin, Minnesota, USA and Milly-la-Forêt, France. In 2017 each line was grown in four
497 replicates and in 2018 in six replicates. Six representative wheat ears were collected from each plot.
498 Additional phenotyping for grains per spike was conducted in Yanco, Milly-la-Forêt and Sabin in 2018
499 and Heading date in Milly-la-Forêt and Sabin in 2018.
500

501 **QTL mapping of SPS**

502 The 4-parent CSIRO MAGIC population had previously been genotyped using both the Infinium 9k and
503 90k SNP chips as well multiple DArTs and microsatellites for key genes[32,33] and the 8-parent NIAB
504 MAGIC population using the Infinium 90k SNP chip[28,34]. QTL analyses were conducted using whole
505 genome average interval mapping using MPWGAIM[33]. For the NIAB MAGIC population a genetic map
506 adapted from Gardner et al., 2016[34] was used. For the CSIRO MAGIC population a previously published
507 map was used[33]. Skimmed genetic maps containing only unique mapping locations were used to

508 calculate MAGIC RIL haplotypes and founder probabilities, and which were then used for QTL mapping
509 using MPWGAIM. Assigned candidate genes are based on previously published allelic information[35].
510

511 **Development of HIF lines and QTL fine mapping**

512 Following the process described by Barrero et al., 2015[31], four founders of heterogeneous inbred
513 families (HIFs) were identified from the F_7 MAGIC RILs through genotyping of the 7AL SPS QTL region
514 using a selection of KASP markers designed based on SNPs from the Infinium iSelect 90K array [63]. After
515 selfing of each (heterozygous) HIF founder, homozygous progeny with contrasting SPS QTL genotypes
516 were selected and self-pollinated to generate sets of contrasting NILs. Plants from four families were
517 then phenotyped across six field trials as described above.

518 Genotyping of the F_{12} lines with the Infinium iSelect 90K array[63] was used to capture any additional
519 recombination in the SPS QTL region and to assign founder genotypes. All NILs were checked and
520 found to contain <1% residual heterozygosity.

521 **7AL and 7BL SPS QTL Candidate gene identification**

522 Candidate genes and their orthologues were initially identified in 2016 based on proprietary gene
523 models. Subsequently the regions have been reannotated with the IWGSCv1.1 gene models as shown
524 in Figure 2. Wheat homoeologues and rice orthologues were identified using Ensembl version 51.
525 Orthologue function was obtained through literature search and from funRiceGenes[64].

526 **7AL and 7BL SPS QTL Candidate gene sequencing**

527 Publicly available *WAPO-A1* and *WAPO-B1* sequences were obtained from the reference wheat line
528 Chinese Spring[41] as well as from Brompton, Robigus and Cadenza (parent of Xi-19)[43]. Additionally, full
529 length sequences for *WAPO-A1* including 5kb upstream promoter sequences in Yitpi, Baxter, Chara
530 and Westonia were obtained via cloning and Sanger Sequencing. Exome sequences for *WAPO1*
531 homoeologues in Alchemy, Claire, Hereward, Rialto, Soissons and Xi-19 were obtained via Exome
532 Capture sequencing.

533 Based on the Chinese Spring reference sequence primers were designed and *WAPO-A1*, *B1* and *D1*
534 sequences were cloned from Chinese Spring, Chara, Baxter, Westonia and Yitpi using a Zero Blunt
535 TOPO Cloning kit (Invitrogen). Subsequently the 5kb promoter sequences for *WAPO-A1* were cloned
536 from overlapping PCRs using the same methodology. Clones were selected on LB + Kanamycin medium
537 and sent for Sanger sequencing after two nights of incubation at 37°C. Sanger Sequencing was
538 performed by LGC (UK). Sequences are available under GenBank accession numbers ON210994 to
539 ON210998. PCR conditions and primers are available in Supplementary Table S6.

540 Wheat Exome Capture sequencing was conducted using a set of internal exome probes based on the
541 IWGSC RefSeqv1 annotations (pre-release) including CDS + UTR sequences. Probe design and
542 balancing was carried out by Roche. Genomic DNA was extracted using a Qiagen DNeasy Mini Kit
543 (Qiagen, US). Library preparation, sequence capture and sequencing were performed at Fasteris.
544 Sequencing was performed on an Illumina HiSeq3000 to obtain an average of 8.2Gb of raw sequence
545 data (2×150bp paired end reads) per sample. Reads for the eight NIAB founders were mapped to the
546 repeat-masked Chinese Spring reference genome (IWGSCv1.0) including mitochondrial (EMBL
547 accession: AP008982) and chloroplast (EMBL accession: AB042240) genomes with BWA[65] (Li, 2013).
548 This includes an additional remapping step to fine-map InDels. Variant calling and filtering were
549 conducted using GATK[66]. Data was stored and accessed through the BiofacetSNP sequence variant
550 data management system.

551 **Candidate gene expression analysis**

552 Chinese Spring developmental time course gene expression data from Choulet et al., 2014[67] for
553 corresponding TGACv1 gene models was accessed on wheat-expression.com[45] in March, 2017. As
554 *WAPO-A1* was not annotated as part of the IWGSC_CSSv2.2[68] and TGACv1 gene models[69] available B
555 and D genome models were used as a query instead.

556 **Gene expression of *WAPO-A1* in the field**

557 Three replicates of whole spike samples were collected from tiller dissections of the 2017 NIAB MAGIC
558 Nursery at growth stage GS32[44] for the MAGIC founders Alchemy, Brompton, Claire, Hereward, Rialto,
559 Robigus and Xi-19. At the collection date Soissons had advanced to GS34. Following dissection, spikes
560 were immediately frozen in liquid nitrogen. For *WAPO-A1,* betaine solution was added at a final
561 concentration of 1M to overcome the amplicons high GC content. To confirm specificity of qRT-PCR
562 reactions the melt curves for each reaction were checked for the presence of only a single peak.
563 Specificity of the assays was confirmed against genomic nullitetrasomic DNA obtained from
564 Seedstor.ac.uk (WPGS1289-PG-1, WPGS1296-PG-1, WPGS1301-PG-1). Expression levels of W*APO-A1*
565 were calculated relative to the expression of the housekeeping genes *TaRP15*[46]and *Ta2291*[47]. Primers
566 sequences are in Supplementary Table S7.

567 ***WAPO-A1* Transformation experiments**

568 A 7,973 bp gene cassette containing the entire Westonia *WAPO-A1* sequence including 5.4 kb of the
569 native promoter was synthetically design at GeneArt (Thermo Fischer Scientific, US) and received in
570 the standard cloning vector pUC57. This cassette was subcloned into the binary vector VecBarII (using
571 the XbaI and HindIII sites), which has been extensively used at CSIRO for wheat transformation[70].
572 CSIRO's Transformation Unit performed the transformation of the Yitpi cultivar or Fielder, using
573 Agrobacterium[71]. Yitpi was chosen over Chara for the complementation experiment because of
574 previous work done at CSIRO showing higher transformation rates in Yitpi (19-27% for Yitpi vs. 5-9%
575 for Chara, data not shown).

576 Thirteen Yitpi and five Fielder primary transformants were generated and grown in pots in the
577 glasshouse. To assess the copy number in each primary transgenic, 25 T_1 seeds from each T_0 plant
578 were germinated in petri dishes and a Basta-resistance 'leaf assay' was used to determine transgene
579 segregation[72]. After a week, the resistance to Basta was scored to determine segregation ratios (data
580 not shown). Based on the segregation ratios six T_0 Yitpi and three T_0 Fielder transformants were
581 selected for further work. From each of them eight T_1 positive lines and two null-segregants were
582 transplanted to soil and grown in glasshouse conditions. For each T_1 plant, about 25 T_2 seeds were
583 used in leaf-tipping assays to identify homozygote lines. A T_2 homozygous and a null-segregant lines
584 from each family were chosen for final analysis. Ten plants of each were transplanted to pots in the
585 glasshouse and they were phenotyped at maturity. Samples were also collected for gene expression
586 analysis in developing spikes.

587 Gene expression of WAPO-A1 in transgenic and control lines was analyzed by RT-qPCR in developing
588 spikes at GS32. Expression levels were calculated relative to the housekeeping gene TaActin1
589 (CJ961169). Primer sequences are in Supplementary Table S7.

All transgenic work was conducted at CSIRO in Canberra (ACT, Australia) in certified Physical Containment Level 2 (PC2) facilities, including laboratories and glasshouses, following the standards set by the Australian Office of the Gene Technology Regulator (https://www.ogtr.gov.au/).

Acknowledgements

CSIRO acknowledges the contributions of Dr Megan N. Hemming, Dr Alex Whan, Dr Richard A. James, Dr Sally Walford and Mr Andrew Spriggs for their support at the early stages of this project. Thanks to Ms Tracy Willis, Mr Jackson Tahapehi, Mr Alexandre Boyer, Dr Aderajew Haddis, Ms Alison Fattore, Ms Bec Maher, Mr David Lewis, Mr Max Bloomfield, Mr Mick Weiss, Mr Patrick Moody and Mr Todd Collins for the management of the field trials at CSIRO. We also thank Ms Terese Richardson and Ms Dhara Bhatt for their work at the CSIRO Wheat Transformation Unit. BASF thanks Xi Wang and Ruvini Ariyadasa for contributions to data analysis early in the work and Greta De Both, Stephanie Thepot, and David Bonnett for management of the field trials at BASF. This project was supported by BASF. Lukas Wittern was funded by BBSRC iCASE grant BB/K011790/1 awarded to Alex Webb (University of Cambridge), Matthew Hannah (BASF) and Andy Greenland (NIAB). Gareth Steed was funded by BBSRC iCASE grant BB/M015416/1 awarded to Alex Webb and Matthew Hannah.

Competing interests

Patent application [73]WO2019/138083 A1 has previously been submitted based on some of these results for which Mark Davey, Colin Cavanagh, Matthew Hannah, Lukas Wittern, Keith Gardner, William Bovill, Jose Barrero and Alex Webb are among inventors. John Jacobs, Mark Davey, Matthew Hannah, Claus Frohberg, Ralf-Christian Schmidt, Colin Cavanagh and Antje Rohde are employees of BASF. Andy Greenland, Gareth Steed, Steve Swain and Trijntje Hughes declare no competing interest.

Data availability

The datasets generated are available for academic partners for non-commercial purposes upon request sent to the corresponding author, provided that bilateral terms-of-use agreements can be concluded.

Author contributions statements

The 4-parent CSIRO MAGIC QTL and HIF work was led by WDB and KLV. JMB and TH did the transgenic analysis. Input on design, analysis and interpretation of results was provided by AR, CC, CF, JJ, MD, MH, RCS and SS. The 8-parent NIAB MAGIC QTL work was conducted by LMW, with gene-expression analysis by LMW and GS. Input on design, analysis and interpretation of results was provided by AARW, KG, AG and MH. LMW and JMB wrote the manuscript. All authors reviewed the manuscript.

624 **Citations:**

625 1. Sreenivasulu, N. & Schnurbusch, T. A genetic playground for enhancing grain number in cereals.
626 *Trends in Plant Science* **17**, 91–101 (2012).
627 2. Zhang, J. *et al.* Identification and validation of QTL for grain yield and plant water status under
628 contrasting water treatments in fall-sown spring wheats. *Theoretical and Applied Genetics* **131**,
629 1741–1759 (2018).
630 3. Li, C. *et al.* Wheat VRN1, FUL2 and FUL3 play critical and redundant roles in spikelet
631 development and spike determinacy. *Development* **146**, dev175398 (2019).
632 4. Shaw, L. M., Turner, A. S., Herry, L., Griffiths, S. & Laurie, D. A. Mutant Alleles of Photoperiod-1
633 in Wheat (Triticum aestivum L.) That Confer a Late Flowering Phenotype in Long Days. *PLOS ONE*
634 **8**, e79459 (2013).
635 5. Brassac, J., Muqaddasi, Q. H., Plieske, J., Ganal, M. W. & Röder, M. S. Linkage mapping identifies
636 a non-synonymous mutation in FLOWERING LOCUS T (FT-B1) increasing spikelet number per
637 spike. *Scientific Reports* **11**, 1585 (2021).
638 6. Shaw, L. M. *et al.* FLOWERING LOCUS T2 regulates spike development and fertility in temperate
639 cereals. *Journal of Experimental Botany* **70**, 193–204 (2019).
640 7. Alvarez, M. A., Tranquilli, G., Lewis, S., Kippes, N. & Dubcovsky, J. Genetic and physical mapping
641 of the earliness per se locus Eps-Am1 in Triticum monococcum identifies EARLY FLOWERING 3
642 (ELF3) as a candidate gene. *Functional & Integrative Genomics* **16**, 365–382 (2016).
643 8. Brinton, J. & Uauy, C. A reductionist approach to dissecting grain weight and yield in wheat.
644 *Journal of Integrative Plant Biology* **61**, 337–358 (2019).
645 9. Li, G., Zhang, H., Li, J., Zhang, Z. & Li, Z. Genetic control of panicle architecture in rice. *The Crop*
646 *Journal* **9**, 590–597 (2021).
647 10. Ikeda, K., Ito, M., Nagasawa, N., Kyozuka, J. & Nagato, Y. Rice ABERRANT PANICLE
648 ORGANIZATION 1, encoding an F-box protein, regulates meristem fate. *The Plant Journal* **51**,
649 1030–1040 (2007).

650 11. Ikeda-Kawakatsu, K. *et al.* Expression Level of ABERRANT PANICLE ORGANIZATION1 Determines
651 Rice Inflorescence Form through Control of Cell Proliferation in the Meristem. *Plant Physiology*
652 **150**, 736–747 (2009).
653 12. Ookawa, T. *et al.* New approach for rice improvement using a pleiotropic QTL gene for lodging
654 resistance and yield. *Nature Communications* **1**, 132 (2010).
655 13. Kim, S.-R. *et al.* Development and validation of allele-specific SNP/indel markers for eight yield-
656 enhancing genes using whole-genome sequencing strategy to increase yield potential of rice,
657 Oryza sativa L. *Rice* **9**, 12 (2016).
658 14. Mizuno, N. *et al.* Genetic mechanisms determining grain number distribution along the spike
659 and their effect on yield components in wheat. *Molecular Breeding* **41**, 62 (2021).
660 15. Ward, B. P. *et al.* Genome-wide association studies for yield-related traits in soft red winter
661 wheat grown in Virginia. *PLoS One* **14**, e0208217–e0208217 (2019).
662 16. Pang, Y. *et al.* High-Resolution Genome-wide Association Study Identifies Genomic Regions and
663 Candidate Genes for Important Agronomic Traits in Wheat. *Molecular Plant* **13**, 1311–1327
664 (2020).
665 17. Würschum, T., Leiser, W. L., Langer, S. M., Tucker, M. R. & Longin, C. F. H. Phenotypic and
666 genetic analysis of spike and kernel characteristics in wheat reveals long-term genetic trends of
667 grain yield components. *Theoretical and Applied Genetics* **131**, 2071–2084 (2018).
668 18. Boeven, P. H. G. *et al.* Genetic architecture of male floral traits required for hybrid wheat
669 breeding. *Theoretical and Applied Genetics* **129**, 2343–2357 (2016).
670 19. Wang, Y. *et al.* Transcriptome Association Identifies Regulators of Wheat Spike Architecture.
671 *Plant Physiology* **175**, 746–757 (2017).
672 20. Su, Z. *et al.* Single nucleotide polymorphism tightly linked to a major QTL on chromosome 7A for
673 both kernel length and kernel weight in wheat. *Molecular Breeding* **36**, 15 (2016).

674 21. Zhai, H. *et al.* QTL Analysis of Spike Morphological Traits and Plant Height in Winter Wheat
675 (Triticum aestivum L.) Using a High-Density SNP and SSR-Based Linkage Map. *Frontiers in Plant*
676 *Science* **7**, 1617 (2016).
677 22. Corsi, B. *et al.* Identification of eight QTL controlling multiple yield components in a German
678 multi-parental wheat population, including Rht24, WAPO-A1, WAPO-B1 and genetic loci on
679 chromosomes 5A and 6A. *Theoretical and Applied Genetics* **134**, 1435–1454 (2021).
680 23. Scott, M. F. *et al.* Limited haplotype diversity underlies polygenic trait architecture across
681 70 years of wheat breeding. *Genome Biology* **22**, 137 (2021).
682 24. Kuzay, S. *et al.* Identification of a candidate gene for a QTL for spikelet number per spike on
683 wheat chromosome arm 7AL by high-resolution genetic mapping. *Theor Appl Genet* **132**, 2689–
684 2705 (2019).
685 25. Muqaddasi, Q. H. *et al.* TaAPO-A1, an ortholog of rice ABERRANT PANICLE ORGANIZATION 1, is
686 associated with total spikelet number per spike in elite European hexaploid winter wheat
687 (Triticum aestivum L.) varieties. *Scientific Reports* **9**, 13853 (2019).
688 26. Voss-Fels, K. P. *et al.* High-resolution mapping of rachis nodes per rachis, a critical determinant
689 of grain yield components in wheat. *Theoretical and Applied Genetics* **132**, 2707–2719 (2019).
690 27. Kuzay, S. *et al.* WAPO-A1 is the causal gene of the 7AL QTL for spikelet number per spike in
691 wheat. *PLOS Genetics* **18**, e1009747 (2022).
692 28. Mackay, I. J. *et al.* An Eight-Parent Multiparent Advanced Generation Inter-Cross Population for
693 Winter-Sown Wheat: Creation, Properties, and Validation. *G3 Genes|Genomes|Genetics* **4**,
694 1603–1610 (2014).
695 29. Scott, M. F. *et al.* Multi-parent populations in crops: a toolbox integrating genomics and genetic
696 mapping with breeding. *Heredity* **125**, 396–416 (2020).
697 30. Arrones, A. *et al.* The Dawn of the Age of Multi-Parent MAGIC Populations in Plant Breeding:
698 Novel Powerful Next-Generation Resources for Genetic Analysis and Selection of Recombinant
699 Elite Material. *Biology* **9**, (2020).

700 31. Barrero, J. M. *et al.* Transcriptomic analysis of wheat near-isogenic lines identifies PM19-A1 and
701 A2 as candidates for a major dormancy QTL. *Genome Biology* **16**, 93 (2015).
702 32. Huang, B. E. *et al.* A multiparent advanced generation inter-cross population for genetic analysis
703 in wheat. *Plant Biotechnology Journal* **10**, 826–839 (2012).
704 33. Verbyla, A. P., Cavanagh, C. R. & Verbyla, K. L. Whole-genome analysis of multienvironment or
705 multitrait QTL in MAGIC. *G3 (Bethesda)* **4**, 1569–1584 (2014).
706 34. Gardner, K. A., Wittern, L. M. & Mackay, I. J. A highly recombined, high-density, eight-founder
707 wheat MAGIC map reveals extensive segregation distortion and genomic locations of
708 introgression segments. *Plant Biotechnology Journal* **14**, 1406–1417 (2016).
709 35. Cane, K. *et al.* Ppd-B1 and Ppd-D1 and their effects in southern Australian wheat. *Crop Pasture*
710 *Sci.* **64**, 100–114 (2013).
711 36. Hyles, J. E. Genome To Phenome: Diversity For Adaptation And Phenology In Wheat (TRITICUM
712 AESTIVUM L.). *Genome To Phenome: Diversity For Adaptation And Phenology In Wheat*
713 *(TRITICUM AESTIVUM L.)* (2021).
714 37. Lee, S., Kim, Y.-Y., Lee, Y. & An, G. Rice P1B-type heavy-metal ATPase, OsHMA9, is a metal efflux
715 protein. *Plant Physiol* **145**, 831–842 (2007).
716 38. Werner, A. K. *et al.* The Ureide-Degrading Reactions of Purine Ring Catabolism Employ Three
717 Amidohydrolases and One Aminohydrolase in Arabidopsis, Soybean, and Rice. *Plant Physiology*
718 **163**, 672–681 (2013).
719 39. Terao, T., Nagata, K., Morino, K. & Hirose, T. A gene controlling the number of primary rachis
720 branches also controls the vascular bundle formation and hence is responsible to increase the
721 harvest index and grain yield in rice. *Theoretical and Applied Genetics* **120**, 875–893 (2010).
722 40. Ando, T. *et al.* Genetic dissection and pyramiding of quantitative traits for panicle architecture
723 by using chromosomal segment substitution lines in rice. *Theoretical and Applied Genetics* **116**,
724 881–890 (2008).

725 41. IWGSC *et al.* Shifting the limits in wheat research and breeding using a fully annotated reference
726 genome. *Science* **361**, eaar7191 (2018).
727 42. Sato, K. *et al.* Chromosome-scale genome assembly of the transformation-amenable common
728 wheat cultivar 'Fielder'. *DNA Research* **28**, dsab008 (2021).
729 43. Walkowiak, S. *et al.* Multiple wheat genomes reveal global variation in modern breeding. *Nature*
730 **588**, 277–283 (2020).
731 44. Zadoks, J. C., Chang, T. T. & Konzak, C. F. A decimal code for the growth stages of cereals. *Weed*
732 *Research* **14**, 415–421 (1974).
733 45. Borrill, P., Ramirez-Gonzalez, R. & Uauy, C. expVIP: a Customizable RNA-seq Data Analysis and
734 Visualization Platform. *Plant Physiology* **170**, 2172–2186 (2016).
735 46. Shaw, L. M., Turner, A. S. & Laurie, D. A. The impact of photoperiod insensitive Ppd-1a mutations
736 on the photoperiod pathway across the three genomes of hexaploid wheat (Triticum aestivum).
737 *The Plant Journal* **71**, 71–84 (2012).
738 47. Paolacci, A. R., Tanzarella, O. A., Porceddu, E. & Ciaffi, M. Identification and validation of
739 reference genes for quantitative RT-PCR normalization in wheat. *BMC Molecular Biology* **10**, 11
740 (2009).
741 48. Mackay, I. J., Cockram, J., Howell, P. & Powell, W. Understanding the classics: the unifying
742 concepts of transgressive segregation, inbreeding depression and heterosis and their central
743 relevance for crop breeding. *Plant Biotechnology Journal* **19**, 26–34 (2021).
744 49. Mathew, B., Léon, J., Sannemann, W. & Sillanpää, M. J. Detection of Epistasis for Flowering Time
745 Using Bayesian Multilocus Estimation in a Barley MAGIC Population. *Genetics* **208**, 525–536
746 (2018).
747 50. Wittern, L. *et al.* Wheat EARLY FLOWERING3 is a dawn-expressed circadian oscillator component
748 that regulates heading date. *bioRxiv* 2021.09.03.458922 (2021) doi:10.1101/2021.09.03.458922.

749 51. Prieto, P., Ochagavía, H., Griffiths, S. & Slafer, G. A. Earliness per se×temperature interaction:
750 consequences on leaf, spikelet, and floret development in wheat. *Journal of Experimental*
751 *Botany* **71**, 1956–1968 (2020).
752 52. Kong, X. *et al.* The wheat AGL6-like MADS-box gene is a master regulator for floral organ identity
753 and a target for spikelet meristem development manipulation. *Plant Biotechnology Journal* **20**,
754 75–88 (2022).
755 53. Andrew Katz *et al.* Identification and Validation of a QTL for Spikelet Number on Chromosome
756 Arm 6BL of Common Wheat (Triticum Aestivum L.). *Molecular Breeding* (2021)
757 doi:10.21203/rs.3.rs-769537/v1.
758 54. Pearce, S., Vanzetti, L. S. & Dubcovsky, J. Exogenous Gibberellins Induce Wheat Spike
759 Development under Short Days Only in the Presence of VERNALIZATION1. *Plant Physiology* **163**,
760 1433–1445 (2013).
761 55. Ikeda-Kawakatsu, K., Maekawa, M., Izawa, T., Itoh, J.-I. & Nagato, Y. ABERRANT PANICLE
762 ORGANIZATION 2/RFL, the rice ortholog of Arabidopsis LEAFY, suppresses the transition from
763 inflorescence meristem to floral meristem through interaction with APO1. *The Plant Journal* **69**,
764 168–180 (2012).
765 56. Selva, C. *et al.* HvLEAFY controls the early stages of floral organ specification and inhibits the
766 formation of multiple ovaries in barley. *The Plant Journal* **108**, 509–527 (2021).
767 57. Huang, Y., Bai, X., Luo, M. & Xing, Y. Short Panicle 3 controls panicle architecture by upregulating
768 APO2/RFL and increasing cytokinin content in rice. *Journal of Integrative Plant Biology* **61**, 987–
769 999 (2019).
770 58. Koppolu, R., Chen, S. & Schnurbusch, T. Evolution of inflorescence branch modifications in cereal
771 crops. *Current Opinion in Plant Biology* **65**, 102168 (2022).
772 59. Glenn, P. *et al.* Identification and characterization of a natural polymorphism in FT-A2 associated
773 with increased number of grains per spike in wheat. *Theoretical and Applied Genetics* (2021)
774 doi:10.1007/s00122-021-03992-y.

775 60. Nakano, H. *et al.* Quantitative trait loci for large sink capacity enhance rice grain yield under
776 free-air CO2 enrichment conditions. *Scientific Reports* **7**, 1827 (2017).
777 61. Huang, L. *et al.* The LARGE2-APO1/APO2 regulatory module controls panicle size and grain
778 number in rice. *The Plant Cell* **33**, 1212–1228 (2021).
779 62. Cullis, B. R., Smith, A. B. & Coombes, N. E. On the design of early generation variety trials with
780 correlated data. *Journal of Agricultural, Biological, and Environmental Statistics* **11**, 381 (2006).
781 63. Wang, S. *et al.* Characterization of polyploid wheat genomic diversity using a high-density 90,000
782 single nucleotide polymorphism array. *Plant Biotechnol J* **12**, 787–796 (2014).
783 64. Yao, W., Li, G., Yu, Y. & Ouyang, Y. funRiceGenes dataset for comprehensive understanding and
784 application of rice functional genes. *GigaScience* **7**, gix119 (2018).
785 65. Li, H. W. Aligning sequence reads, clone sequences and assembly contigs with BWA-MEM. *arXiv:*
786 *Genomics* (2013).
787 66. McKenna, A. *et al.* The Genome Analysis Toolkit: a MapReduce framework for analyzing next-
788 generation DNA sequencing data. *Genome Res* **20**, 1297–1303 (2010).
789 67. Choulet Frédéric *et al.* Structural and functional partitioning of bread wheat chromosome 3B.
790 *Science* **345**, 1249721 (2014).
791 68. IWGSC *et al.* A chromosome-based draft sequence of the hexaploid bread wheat (Triticum
792 aestivum) genome. *Science* **345**, 1251788 (2014).
793 69. Clavijo, B. J. *et al.* An improved assembly and annotation of the allohexaploid wheat genome
794 identifies complete families of agronomic genes and provides genomic evidence for
795 chromosomal translocations. *Genome Res* **27**, 885–896 (2017).
796 70. Richardson, T., Thistleton, J., Higgins, T. J., Howitt, C. & Ayliffe, M. Efficient Agrobacterium
797 transformation of elite wheat germplasm without selection. *Plant Cell, Tissue and Organ Culture*
798 *(PCTOC)* **119**, 647–659 (2014).

71. Ishida, Y., Tsunashima, M., Hiei, Y. & Komari, T. Wheat (Triticum aestivum L.) Transformation Using Immature Embryos. in *Agrobacterium Protocols: Volume 1* (ed. Wang, K.) 189–198 (Springer New York, 2015). doi:10.1007/978-1-4939-1695-5_15.
72. Jacobsen, J. *et al.* Barley (Hordeum vulgare L.). in *Agrobacterium Protocols* (ed. Wang, K.) 171–184 (Humana Press, 2006). doi:10.1385/1-59745-130-4:171.
73. Davey, M. *et al.* Gene underlying the number of spikelets per spike qtl in wheat on chromosome 7a. (2019).